Check for updates

Technoeconomic analysis of metal–organic frameworks for bulk hydrogen transportation†

Aikaterini Anastasopoulou,[a] Hiroyasu Furukawa, [ID] [bc] Brandon R. Barnett, [ID] [bc] Henry Z. H. Jiang,[bc] Jeffrey R. Long [ID] [bcd] and Hanna M. Breunig [ID] *[a]

Numerous adsorption-based technologies are emerging as candidates for hydrogen transportation, and yet little is known about their practical viability. As such, new approaches are needed to conduct early validation of emerging hydrogen transportation concepts despite a lack of clear criteria for viable future hydrogen supply chains. In this work, we conduct technoeconomic modeling to quantify cost, performance, and relations between system components for early-stage adsorbent-based hydrogen supply chains. We compare results with the cost and performance of high pressure compressed gas and liquid hydrogen trucks in the same applications. Using available experimental adsorption data, we simulate the gravimetric performance of tube trailer trucks packed with metal–organic frameworks (MOFs) operated at 100 bar and 77 or 200 K. We also extrapolated available experimental data to study a third scenario where tube trailer trucks are operated at ambient temperature and 250 bar. Models developed for these conditions represent feasible operation scenarios where pressurization or cooling costs can be reduced relative to compressed or liquid hydrogen truck systems. Results suggest that the levelized cost of long-distance transmission, including a gas terminal and MOF-based truck fleet, ranges from $7.3 to $29.0 per kg H_2. The levelized cost of transmission using compressed hydrogen gas trucks at 350 and 500 bar and liquid hydrogen trucks is substantially lower, at $1.8, $1.7 and $3.1 per kg H_2, respectively. In a short-distance urban distribution application, the MOF-based truck fleet, gas terminal, and refueling stations have a levelized cost between $11.8 and $40.0 per kg H_2, which is also more expensive than distribution in the case of the 350 bar, 500 bar and liquid hydrogen trucks, which have levelized costs of $4.7, $4.1 and $3.9 per kg H_2, respectively. Key opportunities identified for lowering costs are: increasing the hydrogen capacity of the tube system by developing new MOFs with higher volumetric deliverable capacities, flexible allowable daily deliveries per refueling station, increasing the cycling stability of the MOF, and driverless trucks.

Broader context

Any path to substantial reduction of greenhouse gas emissions will include market transformations in the transportation sector, which remains the single largest primary source of emissions in the United States and the third-largest global primary emissions source. Advanced porous materials exhibit vast chemical and physical tunability and could radically change the way H_2 is transported around the globe to meet fuel demand in zero direct emission vehicles. This work presents a detailed analysis of the current technology status and cost profile of metal–organic frameworks for H_2 transmission and delivery. The open access models introduced here provide a wealth of information on the viability and outcome expected for using a particular adsorbent in a H_2 transportation application, based on typical experimental data, and capture previously unknown supply chain energy consumption and life-cycle costs. The analysis developed here establishes a foundation for the evaluation of life-cycle costs of emerging H_2 delivery systems and markets and provides guidance for research and prototyping in this area.

[a] *Energy Analysis and Environmental Impacts Division, Lawrence Berkeley National Laboratory, Berkeley, CA, 94720, USA. E-mail: hannabreunig@lbl.gov*

[b] *Department of Chemistry, University of California, Berkeley, CA, 94720, USA*

[c] *Materials Sciences Division, Lawrence Berkeley National Laboratory, Berkeley, CA, 94720, USA*

[d] *Department of Chemical and Biomolecular Engineering, University of California, Berkeley, CA, 94720, USA*

† Electronic supplementary information (ESI) available: Details and results of the modeling and technoeconomic analysis of hydrogen delivery. See DOI: 10.1039/d0ee02448a

Introduction

The role of hydrogen (H_2) as an energy carrier has become increasingly important in decarbonizing the global energy sector.[1–3] Hydrogen can be synthesized from a broad range of energy resources and has a higher energy content per unit mass than gasoline or natural gas, making it an attractive alternative fuel for various on-board applications. However, one of the greatest technical challenges facing the accelerated deployment

This journal is © The Royal Society of Chemistry 2021

Energy Environ. Sci., 2021, **14**, 1083–1094 | **1083**

of H_2 is the cost of storage and transport, due to its poor volumetric energy density (0.01 MJ L^{-1} at ambient conditions).[4–6]

Compressed hydrogen gas, hereafter referred to as Comp-H_2, is widely used today for H_2 transportation in industry; however, gas pressures at ambient temperature are restricted to between 160 and 400 bar, and therefore only modest amounts of H_2 can be carried based on tank size and bulk density (<700 kg H_2). Consequently, this well-established technology is unsuitable for serving the large refueling stations (>1000 kg) that could potentially supply and enable growth in light-duty fuel cell vehicles or for transporting H_2 over long distances.[7] Liquefied H_2 (Liq-H_2) can serve large refueling stations, but liquefaction is energetically costly and subject to product losses via boil-off and pumping, which may be considered prohibitive disadvantages in certain applications.[8,9]

In the last two decades, much effort has been devoted to the design and synthesis of highly porous adsorbents for potential H_2 storage applications.[4,6,10] Many of these materials can store greater amounts of H_2 at lower pressures than conventional high-pressure gas cylinders, and metal–organic frameworks (MOFs) in particular have garnered substantial interest. Consisting of inorganic clusters bridged by organic linkers, MOFs exhibit substantial chemical and structural diversity as well as high specific surface areas, often of greater than 1000 m^2 g^{-1}. While a vast number of materials have been investigated theoretically and experimentally for H_2 physisorption,[4,10,11] it is challenging to assess their potential performance in real-world applications. Few studies to date have provided preliminary assessment of system-level costs for adsorbent-based hydrogen storage, including energy and material balances, or determined bounds on variability in key system parameters and their interactions.[12,13] In a future where hydrogen plays a prominent global role in energy storage, renewable energy integration, resilience, transportation, and industry, there will be cases where hydrogen can be generated at the point of use, and cases where hydrogen must be stored and transported in one form or another from the point of production to the point of use. The costs associated with existing bulk H_2 transportation systems involve pipelines, Comp-H_2 and Liq-H_2 based trucks have been widely investigated and can be applied to estimate the cost of H_2 for these applications.[19–23] However, the values and assumptions used to model the H_2 supply chain vary among studies and are not always reported in literature where the emphasis is placed on either the source or use of the H_2 itself. The lack of simple, open access tools for modeling logistics and transportation makes it challenging to construct fair comparisons between incumbent and emerging technologies.

Motivated by this research need, in this study we couple process simulations of system components, truck logistics models, and bottom-up discounted cash flow analysis in a novel prospective technoeconomic analysis (TEA) of MOF-based H_2 delivery. More specifically, cost and performance in geographically agnostic value chains for Comp-H_2 tube trailers (350 and 500 bar),[14,15] Liq-H_2, and MOF-H_2 transportation methods are evaluated using the same system boundaries for

a reasonable comparison. Given the importance of low-cost "last-mile" delivery options for shuttling H_2 from a port, rail station, or city-gate dehydrogenation facility to distributed refueling stations,[8] we discuss different scenarios to realize cost-effective solutions for both long-distance transmission and short-distance (last mile) distribution value chains (Fig. 1).

Two prototypical MOFs were chosen to serve as representative adsorbents, namely $Zn_4O(bdc)_3$ (MOF-5; bdc^{2-} = 1,4-benzenedicarboxylate)[16] and $Ni_2(m\text{-dobdc})$ ($m\text{-dobdc}^{4-}$ = 4,6-dioxido-1,3-benzenedicarboxylate).[17] MOF-5 can be prepared with a Brunauer–Emmett–Teller surface area as high as 3800 m^2 g^{-1} and exhibits high usable gravimetric and volumetric capacities of 4.5 wt% H_2 and 31.1 g H_2 per L, respectively, between 5 and 100 bar at 77 K.[11,18] These capacities are notably 18% and 77% higher than that of Comp-H_2 at 350 bar and room temperature. The framework $Ni_2(m\text{-dobdc})$ is currently the top-performing adsorbent for near ambient temperature H_2 storage and features a high density of coordinatively unsaturated Ni^{2+} sites that strongly bind H_2 (binding enthalpy = -13.7 kJ mol^{-1}). The usable volumetric capacity of $Ni_2(m\text{-dobdc})$ is 23.4 g H_2 per L between 5 and 100 bar with a temperature swing between -75 and 25 °C.[19]

The prospective analysis developed here establishes ranges for the potential performance of H_2 delivery technologies that could be expected under realistic operating conditions and scales, and identifies factors that could significantly lower upfront and life-cycle costs. The knowledge generated in this study is intended to guide research decisions made by material scientists and process engineers, as reverse engineering a MOF-based H_2 delivery technology that is cost competitive with Comp-H_2 or Liq-H_2 in these applications goes beyond setting targets for system gravimetric and volumetric capacities.

Methods and materials

The performance and cost of Comp-H_2, Liq-H_2, and MOF-H_2 delivery technologies were first estimated for two plausible H_2 transportation supply chains at the scale of 50 000 kg H_2 per day (see Fig. 1). The first supply chain is "point-to-point" long-distance transmission (100 km). In this scenario, it was assumed that H_2 is produced renewably by water splitting at a 1 GW equivalent facility (610 000 kg H_2 per day)[20] that has one days' worth of above-ground Comp-H_2 storage at the terminal where trucks pick up H_2. Such large renewable H_2 production facilities are unlikely to be co-located with industrial or urban markets, making H_2 transportation necessary.

The second supply chain is "last mile" inner-city (1 km) distribution, and here it was assumed that pure H_2 is delivered to the city-gate terminal from a pipeline. We also assumed pure H_2 is provided to the gas terminals, and additional pre-treatment for possible trace gases is not considered. Given that large-scale H_2 trucking infrastructure including these terminals do not presently exist, we developed a novel methodology to describe specific system components, their interactions, and operation patterns by integrating data from literature, existing H_2 delivery

1084 | Energy Environ. Sci., 2021, 14, 1083–1094

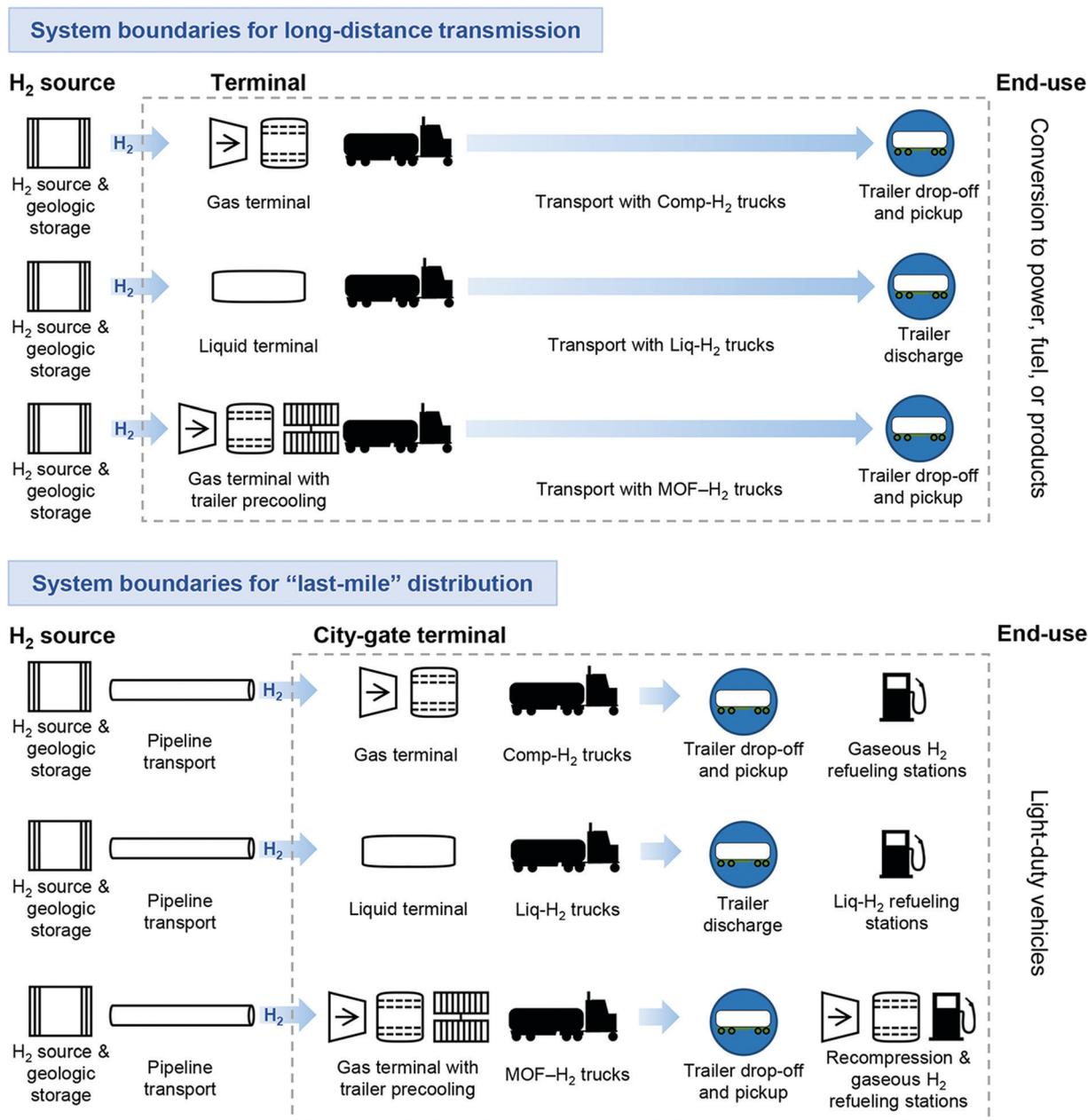This journal is © The Royal Society of Chemistry 2021

Fig. 1 Illustration of the system boundaries of the technoeconomic analysis presented in this study and used to compare the performance of hypothetical MOF-H$_2$ transportation technologies with incumbent compressed hydrogen gas (Comp-H$_2$) and liquid hydrogen (Liq-H$_2$) technologies. Process models, energy balances, and cost estimates were derived within these boundaries. The approach is demonstrated for two hydrogen transportation supply chains: long-distance "point-to-point" transmission and "last-mile" inner-city distribution using on-road trucking systems. Truck systems consist of Comp-H$_2$, Liq-H$_2$, and MOF-H$_2$ trucks, all equipment required for loading H$_2$ onto trucks at the H$_2$ source terminal or city-gate terminal, and the refueling stations. In the long-distance transmission supply chain, H$_2$ is delivered to a gas or liquid terminal at 20 bar and 294 K. In "last-mile" distribution supply chain, H$_2$ is delivered to the city-gate terminal at 48 bar and 298 K. Refueling station storage systems are assumed to operate at 350 bar and 298 K. Importantly, the tools developed here enable the analysis of the practical viability of any MOF system in the literature for H$_2$ transport applications, using adsorption data alone.

modeling tools, and analogous processes with our own models. A brief description of our methodology and assumptions are presented in this section, with further details provided in Section 1 of the ESI.†

In addition to modeling the two supply chains, we ran a sensitivity analysis on uncertain parameters, including adsorption

system parameters (durability, bulk density, and precooling requirements), material and equipment costs, logistic parameters (driverless trucks, flexible refueling stations that allow for two deliveries per day) and market characteristics (distance and scale). We evaluated the impact of driverless trucks on overall costs, as the trucking industry is expected to become an early adopter of

This journal is © The Royal Society of Chemistry 2021

Energy Environ. Sci., 2021, **14**, 1083–1094 | **1085**

autonomous vehicle technology, which can improve safety, lower tailpipe emissions, and minimize labor costs.[21,22] We further considered a third supply chain scenario ("transmission-distribution") where the same truck fleet delivers H_2 over long distances and into the city to refueling stations. Finally, we explored whether increasing the maximum adsorption capacity in a MOF-based system is enough to reach cost parity with Comp-H_2 and Liq-H_2 systems for H_2 delivery.

Adsorption (MOF-H_2) tube-trailer model

The MOF-H_2 system is represented assuming tube trailers containing nine separate Type III pressure vessels (tubes),[6,23–25] where each tube is filled with MOF packing material (pellets) and is modeled as a packed bed with the design specifications shown in Table 1.

In the absence of prototype adsorption column data, we estimated the amount of adsorbent and adsorbed H_2 per truck by modeling the packed bed in MATLAB software (see Section 1.2 of the ESI† for details).[26] This approach required an approximation for the material bulk density, also known as packing density, in the pressurized tubes. Bulk density is critical for the adsorption performance[27–29] and is a function of both bed porosity, ε_b, and pellet porosity, ε_p; we approximated bulk density as the product $\rho_{bulk} = (1 - \varepsilon_b) \cdot (1 - \varepsilon_p) \cdot \rho_s$, where ρ_s is the MOF single crystal density. We were unable to obtain experimental data for the two studied MOFs that captures mass transfer phenomena and illustrates the net effect of particle size on adsorption efficiency. Instead, our analysis assumes a particle size of 1 μm, which approximates the particle size for which experimental data on H_2 uptake are typically measured.[30] A brief analysis on the impact of larger particle size (1 mm) on the examined adsorption systems and a discussion on the challenges associated with such design considerations is provided in Section 6 of the ESI.† A dual-site Langmuir isotherm model was used to estimate the total H_2 uptake and to fit available experimental H_2 adsorption data up to 100 bar at 77 and 200 K for MOF-5 (Fig. S1, ESI†) and at temperatures ranging from 77 to 372 K for Ni$_2$(m-dobdc) (Fig. S2 and S3, ESI†).[18,19] The analysis in this work is focused primarily on the performance of both MOF systems at 77 and 200 K and 100 bar, due to the maximum H_2 capacity attained at that pressure, the feasibility of designing trucks for these operation conditions, and the importance of lowering parameter uncertainty by using experimentally verified data. An additional exploratory case study is also

examined at 298 K and 250 bar for the Ni$_2$(m-dobdc) system, given the available isotherm data at ambient temperature for this MOF (Section 1.2 of ESI†). It is important to note that the operating conditions presented here were selected for a proof-of-concept exploration of the advantages of these two particular MOF-based systems over Liq-H_2 and Comp-H_2 under conditions where H_2 uptake is maximized or compression and cooling costs are minimized. Strategies aimed at developing new MOFs that exhibit enhanced deliverable H_2 storage capacities and operating temperatures continue to be key materials science objectives that will undoubtedly lead to further refinement and optimization of system boundaries for real-world applications.

The amount of desorbed H_2 and the discharging time were estimated based on the same adsorption model. Ultimately, these time variables are not considered as constraints on driver and truck availability, or as barriers for technology application in the studied supply chains, due to the possibility of trailer switching at end points and refueling stations. As a result, our model prioritizes energy and cost savings and assumes a depressurization process for desorption, as opposed to a faster but more complex temperature swing process.

Modeled capacities and tube adsorption/desorption times are presented in Table S7 (ESI†) for "base case" as well as "low packing density" and "high packing density" scenarios. The results presented below in general refer to the base case scenario, and variations considered for low and high packing density scenarios are specified where relevant. In addition to the design specifications for the tube trailers (Table 1), the base case scenario assumes a MOF pellet cost of $10 per kg,[31] material stability for 5000 adsorption cycles,[32] and a delivery rate of 50 000 kg H_2 per day. Although various approaches could be explored for recovery of the MOF from the tube trailers, an end-of-life analysis of MOF-packed tubes was not performed in this study, and thus it is assumed that the whole tube-trailer must be replaced when the MOF packing material expires. This assumption is conservative but reasonable given tubes tend to be mounted on trailers and a trailer would necessarily go offline, even temporarily, if an adsorbent material could somehow be recovered.

Compressed and liquid H_2 (Comp-H_2 and Liq-H_2) tube-trailer model

We modeled the Comp-H_2 system assuming tube trailers with nine distinct Type IV pressure vessels at 350 or 500 bar.[6,25] At these pressures, the trucks can store a maximum of 630 and 800 kg H_2, respectively, and deliver 95% of this storage capacity.[14,33] We assumed the maximum storage capacity of the Liq-H_2 system to be 4082 kg H_2 per truck at cryogenic conditions based on relevant literature data.[34]

Gas terminal and refueling station model

The equipment and operation of the gas terminal includes storage, refrigeration, and compression units, as determined based on our process simulations run in ProSim software (see Section 1 of the ESI† for details).[35] This model considers one truck delivery per day and thus refueling station capacity is determined from the truck

Table 1 "Base case" design specifications for hypothetical H_2 storage tubes packed with MOF for use on truck-trailers delivering H_2

Process parameter	Value	Ref.
Tube length, L_{tube} (m)	12	23
Tube diameter, d_{tube} (m)	0.56	23
Bed length, L (m)	$0.9 \times L_{tube}$	This study
Bed diameter, d (m)	$0.9 \times d_{tube}$	This study
Pellet porosity, ε_p	0.2	This study
Bed porosity, ε_b	0.6	This study
Gas flow rate, Q (m^3 s^{-1})	0.001	This study
MOF particle diameter, D_p (m)	1×10^{-6}	This study

1086 | *Energy Environ. Sci.*, 2021, **14**, 1083–1094

This journal is © The Royal Society of Chemistry 2021

systems models. As such, gaseous H_2 refueling station capacities were assumed to range from 100 to 300 kg H_2 per day for the MOF-H_2 systems, 600 and 800 kg H_2 per day for the 350 and 500 bar Comp-H_2 systems, respectively, and 3000 kg H_2 per day for Liq-H_2. We modeled the refueling stations using the Hydrogen Refueling Station Analysis Model (HRSAM) from Argonne National Laboratory.[36]

Truck logistics-model

Following the assessment of H_2 capacity for each tube-trailer type and refueling station, we estimated the relative number of truck cabs, trailers, and refueling stations necessary for each method of H_2 delivery based on our assumed daily H_2 demand, truck operation and availability, and end-point capacity factors. In this analysis, the approach applied was analogous to that reported previously for modeling the following trucking logistics.[8] For Comp-H_2 and MOF-H_2 truck fleets, it is expected that a driver will exchange a full tube-trailer for a waiting, empty trailer. This assumption is realistic, given that Comp-H_2 tube trailers can be employed as part of the refueling station storage system; switching trailers also limits driver waiting time. Liq-H_2 tanker trucks remain with their cabs and discharge fully before returning to the terminal, in order to lower product losses and minimize the required number of Liq-H_2 tanks.

Cost model

Life-cycle costs for each H_2 delivery system include all capital and operating expenditures over a 30-year period, which was selected based on the target lifespan of main process equipment, such as the liquefier and storage tanks.[37] We assumed 357 days of operation per year, an inflation rate of 1.9%, and a tax rate of 38.9%.[14] All costs were adjusted to a 2020 dollar value in a discounted cash flow analysis using a Modified Accelerated Cost Recovery System depreciation cost approach.[14] The cost of the trucks themselves, including specific tube configuration costs, were derived from the Tankinator tool developed by the Hydrogen Storage Engineering Center of Excellence (HSECoE).[24] The operating costs for the truck, including labor and maintenance, were modeled based on 2017 comprehensive data compiled by the American Transportation Research Institute.[38] Capital and operating costs for the gas terminals and refueling stations are provided in Section 1.4 of the ESI.† The levelized cost of H_2 delivery at a set market size was estimated by dividing the annual capital and operating costs by the annual delivered H_2 amount ($ per kg). The levelized cost of H_2 delivery per truck was estimated by dividing the annualized capital costs of the truck system by the annual delivered H_2 amount per truck ($ per kg). Variations to input capital and operating costs, including the cost of MOF pellets ($5 to $15 per kg pellets),[39] are reflected in the error bars shown in Fig. 3 and 4.

Sensitivity analysis and model benchmarking

A sensitivity analysis was performed to quantify how variable and uncertain parameters affect the modeled performance of the MOF-H_2 delivery technology. The adsorption system parameters examined in this analysis were MOF durability (5000 to 15 000 cycles),[40–42] input cost values (±50%) (Table S6, ESI†), and the bulk densities of MOF-5 and Ni$_2$(m-dobdc) (0.04–0.34 and 0.07–

0.67 g cm^{-3}, respectively). Varied market parameters were distribution distance (1 to 50 km), transmission distance (25 to 300 km), and scale or daily H_2 demand (2000 to 120 000 kg H_2 per day). Base values for MOF cost, density, and durability were derived from the literature and correspondence with members of the HSECoE and industry stakeholders. These quantities represent current state of the art in MOF adsorption systems.[43] It is important to note that this analysis is intended as a benchmarking study, and ranges in the cost parameters are arbitrary and included solely for understanding the robustness of the results.

For data consistency purposes, the Hydrogen Delivery System Analysis Model (HDSAM) developed at Argonne National Laboratory was used to benchmark our results for the 500 bar Comp-H_2 system (see Section 4 of the ESI†). The models are in good agreement and we determined a levelized cost for the combined transmission–distribution value chain that is only 2% greater than that determined using HDSAM.

Results and discussion

Adsorption column performance

A dual-site Langmuir model was used to fit experimental isotherm data for MOF-5 and Ni$_2$(m-dobdc) (Fig. S1–S3 and Table S2, ESI†).[18,19] Values for the H_2 heat of adsorption, Q_{st}, in both frameworks were extracted from the literature and are assumed to be temperature-independent (see Section 1.4.1 of the ESI†).[17,44] Using the adsorption model presented in Section 1.2 of the ESI,† saturation simulations were performed to estimate the time to reach 95% saturation and the amount of H_2 adsorbed in the MOF-filled tubes. In addition to the packing density considered in the base case scenario ($\varepsilon_b = 0.6$; $\varepsilon_p = 0.2$), we also simulated saturation for high ($\varepsilon_b = 0.3$; $\varepsilon_p = 0.2$) and low ($\varepsilon_b = 0.7$; $\varepsilon_p = 0.8$) bulk density scenarios. Selected saturation curves are presented in Fig. 2 for a Ni$_2$(m-dobdc) truck and in Fig. S4 (ESI†) for a MOF-5 truck, and all data are summarized in Table S7 (ESI†) for both materials.

When operated at 77 K, the base case Ni$_2$(m-dobdc) truck ($\rho_{bulk} = 0.38$ g cm^{-3}) requires 50 min to charge to capacity (300 kg of H_2) when the tubes are charged in parallel (Fig. 2, blue curve). When operated at 200 K, the same truck requires 37 min to charge to capacity at $\sim$65 kg H_2 (Fig. 2, orange curve). For a high bulk density Ni$_2$(m-dobdc) bed operated at 200 K ($\rho_{bulk} = 0.67$ g cm^{-3}), H_2 adsorption takes place in 49 min to reach a capacity of $\sim$154 kg H_2 (Fig. 2, dark orange curve). For the low bulk density scenario ($\rho_{bulk} = 0.07$ g cm^{-3}), the truck can be charged to capacity at $\sim$30 kg H_2 in only 16 min (Fig. 2, pale orange curve). Packing density and saturation time shows a clear nonlinear trend as expected.[45] In the case of high packing density, longer residence time is required to attain saturation due to the smaller void space and the increased adsorbent mass.[46–48] Moreover, the sluggish saturation curve for the high packing density scenario in Fig. 2 can be attributed to the expanded mass transfer zone, which is a function of several operating parameters, including diffusion rate, adsorption isotherm, and mass transfer rate.[45]
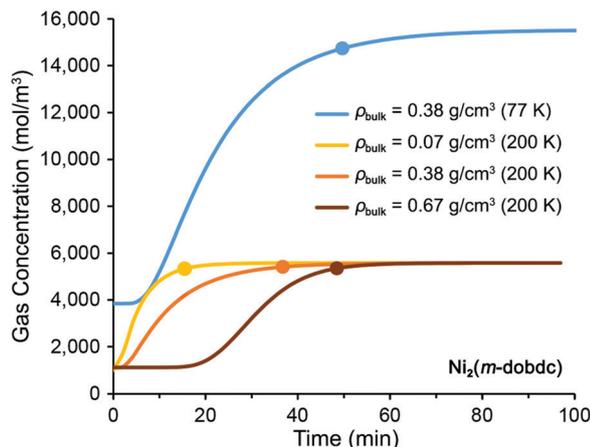
This journal is © The Royal Society of Chemistry 2021

Energy Environ. Sci., 2021, **14**, 1083–1094 | **1087**

Fig. 2 Simulated gas-phase concentration saturation curves for H_2 adsorption in $Ni_2(m\text{-dobdc})$. Filled circles indicate 95% saturation. Initial non-zero concentrations (at $t = 0$) denote that tubes are not fully emptied during discharge cycles.

Similar results were obtained from saturation simulations with MOF-5 truck beds (see Fig. S4 and Table S7, ESI†). For the 200 K medium density case, a MOF-5 truck charges to capacity at ∼61 kg H_2 in 31 min, thus the charging time is slightly less than the $Ni_2(m\text{-dobdc})$ base case, but the total H_2 adsorbed is also less. At 77 K, the MOF-5 system capacity is 7% more than that with $Ni_2(m\text{-dobdc})$ in the same adsorption time. As seen for $Ni_2(m\text{-dobdc})$, lower and higher MOF-5 packing densities are associated with faster and slower charging times, respectively, relative to the medium density case (Table S7, ESI†). Finally, while adsorption times are not considered to be a barrier in these market applications if tube-trailer switching is feasible, our model captures the clear trade-off between refueling time and H_2 uptake.

System-level energy penalties

For the transmission delivery mode using Comp-H_2, compression costs represent the sole energy consumption at the gas terminals and constitute 12 and 14% of the total delivered H_2 energy content for trucks carrying 350 and 500 bar Comp-H_2, respectively (Table S4, ESI†). Adsorption-based systems incur additional energy penalties beyond those associated with gas compression at the terminal. First, it is highly likely that MOF-packed beds will need to undergo pre-cooling to enhance adsorption efficiency. As we assume a truck driver exchanges a waiting tube-trailer for an empty one at the terminal, we do not assume the precooling step affects the amount of time that the driver can be on the road. The importance of considering precooling is evident when modeling the energy penalties and running costs of an adsorption based technology, although precooling has not been widely acknowledged in the literature as a potential disadvantage to adsorbent-based technology.[49,50] Including precooling the trailers waiting to be filled, the energy required at the gas terminals for $Ni_2(m\text{-dobdc})$ and MOF-5 systems operating at 200 K is estimated to be 43% and 32%

of the H_2 energy content, which is comparable with the energy penalties expected for liquefaction (Table S4, ESI†). The low-temperature Comp-H_2 gas terminal used to fill the MOF trucks is more energy intensive than the liquefaction terminal, as it must use refrigeration systems for both precooling of the bed and to remove the heat generated upon adsorption. For a MOF-based system operating at 77 K, the energy costs are even more substantial, and cooling 50 000 kg H_2 per day would require considerable energy beyond that from the delivered hydrogen.

It is assumed that Comp-H_2 systems require only one compression step at the gas terminal, given that the refueling station is operated at 350 bar and it is expected that the Comp-H_2 trailer will serve as part of the refueling station storage system (see Section 1.1 of the ESI†).[51–53] For the MOF-based trucks, H_2 is first compressed to 100 bar for transportation at the gas terminal (Table S4, ESI†) and then re-pressurized after desorption for transfer to the refueling station storage vessels (350 bar and 298 K) which can rapidly provide H_2 at pressure, as modeled in HRSAM (Table S5, ESI†).[36] Even if the MOF-packed trailer were to serve as part of the refuelling station storage system, a repressurization step after desorption would be necessary. Energy costs for re-pressurizing H_2 up to 350 bar from the MOF tube trailers represent 20–25% and 4–18% of the delivered H_2 energy content at 200 and 77 K, respectively, not including capital costs. Allowing the cold MOF-based trucks to warm or applying heat for desorption, rather than employing a pressure swing, could reduce recompression costs at the refueling station, but would yield additional recooling costs at the gas terminal. These scenarios were excluded from this initial analysis and will be considered in a future study. Analogous to the Comp-H_2 systems, Liq-H_2 trucks are assumed to deliver H_2 at the operating conditions of the Liq-H_2 refueling station, as modeled in HRSAM.[36]

Hydrogen transmission delivery costs

In the transmission supply chain, total costs are attributed to capital and operating costs over a 30-year timespan for a single gas terminal and a truck fleet transiting from the terminal to one or more non-refueling station end points. The levelized costs (and individual cost contributions) as determined for Comp-H_2 and Liq-H_2 systems are presented in Fig. 3 for delivery of 50 000 kg H_2 per day. Our results suggest the long distance (100 km) transmission of 50 000 kg H_2 per day would require 43 Comp-H_2-350 bar trucks or 34 Comp-H_2-500 bar trucks at a levelized cost of \$1.8 and \$1.7 per kg H_2, respectively. In this scenario, 57% and 62% of the levelized cost is allocated with the gas terminal. The 500 bar Comp-H_2 system enables the transportation of 29% more hydrogen per truck compared to the 350 bar system, but this aspect is not proportionally reflected in the final delivery cost, due to the high capital cost of the gas compression units. Delivery using the Liq-H_2 system would require only 13 trucks at a levelized cost of \$3.1 per kg H_2, with 93% of the levelized cost attributed to the liquefaction terminal.
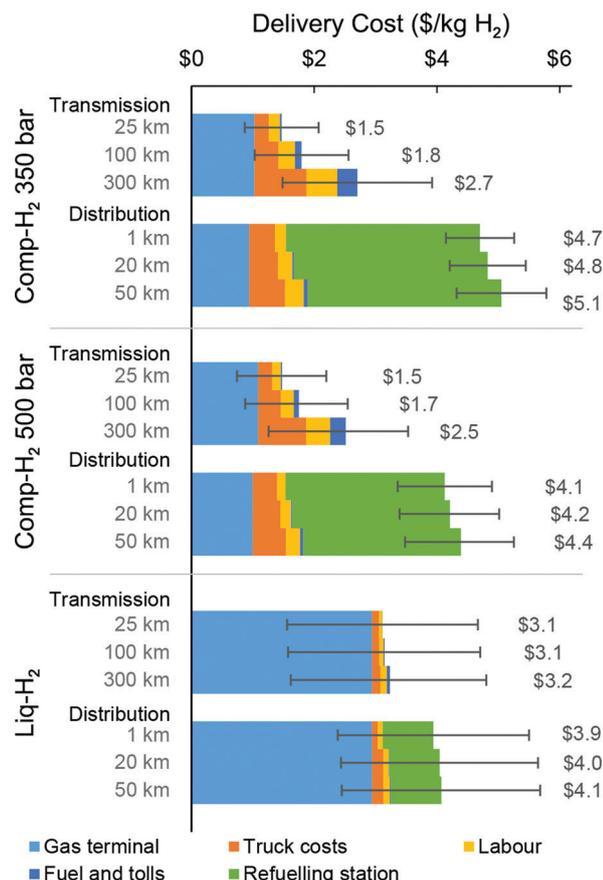
1088 | *Energy Environ. Sci.*, 2021, **14**, 1083–1094

This journal is © The Royal Society of Chemistry 2021

Fig. 3 Hydrogen cost profiles for Comp-H_2 and Liq-H_2 delivery systems for 50 000 kg H_2 per day (see Fig. S5, ESI† for variations in the costs for delivery rates ranging from 2000 to 120 000 kg H_2 per day). Base driving distances are shown for transmission (100 km) and distribution (1 km) supply chains, along with variations. Error bar lower and upper bounds reflect a 50% decrease and increase in input capital and operating costs, respectively. The number of trucks involved in each H_2 delivery system is presented in Table S3 (ESI†).

Fig. 4 Hydrogen cost profiles for MOF-H_2 delivery systems for 50 000 kg H_2 per day (see Fig. S5, ESI† for variations in the costs for delivery rates ranging from 2000 to 120 000 kg H_2 per day). Base driving distances are shown for transmission (100 km) and distribution (1 km) supply chains, along with variations. Error bar lower bounds reflect a 50% decrease in input capital and operating costs and an assumption that tube trailers can be precooled from an initial temperature of 87 K. Error bar upper bounds reflect a 50% increase in the input capital and operating cost values and "cold start-up" where tube trailers must be precooled from an initial temperature of 298 K. The number of trucks involved in each H_2 delivery system is presented in Table S3 (ESI†).

Cost analysis results for the MOF-H_2 systems at 77 and 200 K are shown in Fig. 4. Notably, the benefit of the higher H_2 adsorption capacities achieved at 77 K outweighs the energy cost of operating at this lower temperature. Long-distance transmission of 50 000 kg H_2 per day using adsorbent systems at 77 K would require 170 Ni$_2$(m-dobdc) trucks at a levelized cost of $10.0 per kg H_2 or 122 MOF-5 trucks at a levelized cost of $7.3 per kg H_2. In contrast, 200 K operation would require 1164 Ni$_2$(m-dobdc) trucks at a cost of $23.5 per kg H_2 or 1551 MOF-5 trucks at a cost of $28.9 per kg H_2. Notably, the gas terminal cost alone for the 77 K MOF-based systems is greater than the full supply chain cost for both Comp-H_2 scenarios, suggesting that even with significant improvement to MOF performance at 77 K, the technology is not competitive with Comp-H_2. Given that truck-related expenses constitute a large percentage of the total levelized cost for the 200 K MOF-H_2 systems, advances capable of increasing the deliverable H_2 capacity of the MOF-packed tube trailers and therefore reducing the number of trucks required are of significant interest.
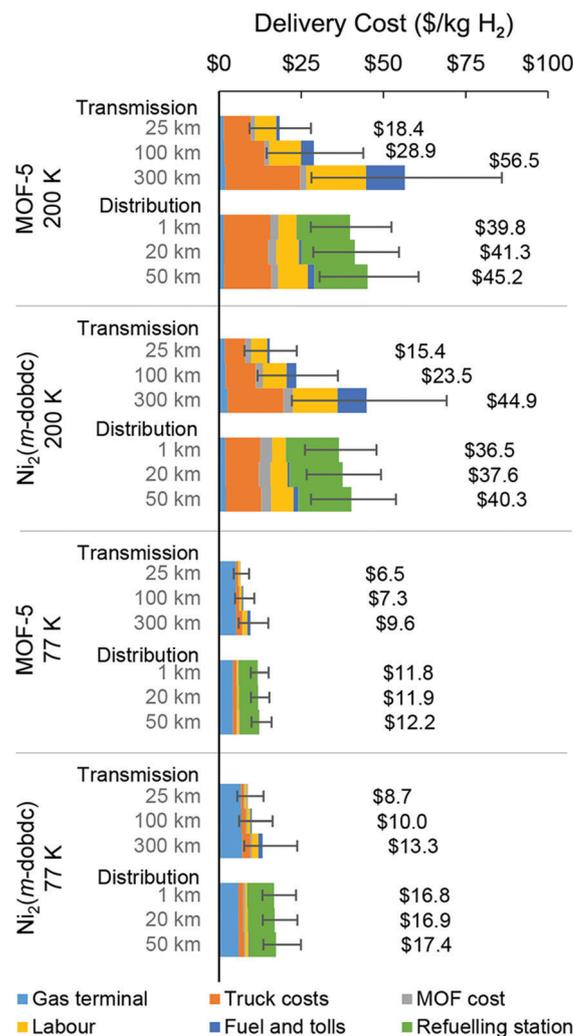
Finally, as the transmission distance increases, the number of Comp-H_2 and MOF-based trucks required to deliver the same quantity of H_2 increases, due to limitations on the hours a driver can operate. In the case of Liq-H_2, the truck number remains constant for all examined distances due to the high H_2 capacity per truck.

Hydrogen distribution delivery costs

The cost profile of Comp-H_2 trucks deployed for "last-mile" delivery is dominated by the cost of the gas terminal and operation of the refueling stations (Fig. 3). For 1 km distribution, refueling station costs account for 67 and 63% of the total

This journal is © The Royal Society of Chemistry 2021

Energy Environ. Sci., 2021, **14**, 1083–1094 | **1089**

levelized distribution costs for the 350 and 500 bar Comp-H$_2$ systems ($4.7 and $4.1 per kg H$_2$, respectively). In contrast, the Liq-H$_2$ system can serve much larger refueling stations, thus requiring fewer stations to meet a set H$_2$ market size. Only 21% of the levelized cost of 1 km Liq-H$_2$ delivery ($3.9 per kg H$_2$) is attributed to the refueling stations. While the Comp-H$_2$ and Liq-H$_2$ systems have comparable levelized costs, the different cost contributions highlight distinct opportunities for cost reductions for each technology.

The current cost of distributing H$_2$ using MOF-based trucks (Fig. 4) is substantially higher than when using Comp-H$_2$ and Liq-H$_2$ trucks. The cost profile for both MOF-5 and Ni$_2$(m-dobdc) is dominated by the high number of trucks and refueling stations required, assuming only one H$_2$ delivery per day is allowed at the refueling station and assuming a station size based on the delivered capacity of one MOF truck. For the 200 K systems, the levelized cost of 1 km distribution is estimated to be $36.5 per kg H$_2$ for Ni$_2$(m-dobdc) and $39.8 per kg H$_2$ for MOF-5 (Fig. 4). Given a dispensing rate of only 100 kg H$_2$ per day (serving ∼20 light-duty fuel cell cars at 5 kg H$_2$ tank capacity), these small refueling stations are expensive as they rely on equipment that benefit from economies of scale. Additionally, because the number of truck trailers is influenced by the number of refueling stations, a very large truck fleet is required. At 77 K, the distribution cost is reduced to $16.8 per kg H$_2$ for Ni$_2$(m-dobdc) and $11.8 per kg H$_2$ for MOF-5, with refueling stations sized at 200 and 300 kg H$_2$ per day, respectively. Considering cost and dispensing capacity, the 200 K MOF systems are clearly the least favorable of all the delivery methods studied here. For Comp-H$_2$, Liq-H$_2$, and MOF-H$_2$, the effect of distance on the distribution cost is modest.

Opportunities for cost reduction

Various scenarios beyond the base case were additionally considered for reducing upfront capital costs, operation and labor costs, and inefficiencies along the studied supply chains for the MOF-H$_2$ systems analyzed here. These data are presented in Fig. 5 and compared with the base case results for each technology and supply chain. For example, in the case of Ni$_2$(m-dobdc) we find that simply by extending the lifetime of the tube trailer from 5000 to 7000 or 15 000 cycles, it is possible to attain a reduction of the H$_2$ transmission costs by 7% and 13%, respectively (blue markers), and distribution costs by 5% and 18%. In addition to increasing the number of MOF cycles, the decoupling of the MOF and tube trailer replacement will help reduce these truck-related costs, particularly for the distribution case. The use of high packing density (HPD) tubes (all other base case conditions held constant) results in even more dramatic reductions in the levelized transmission and distribution costs, by as much as 80% and 73%, respectively, in the 200 K MOF-5 scenario. With these engineering improvements, the levelized transmission cost of the MOF-H$_2$ systems becomes lower than that of the Liq-H$_2$ system and comparable with the Comp-H$_2$ systems. These cost reductions do not reflect a theoretical minimum, but a minimum that is bounded by the adsorption properties of the materials evaluated here,
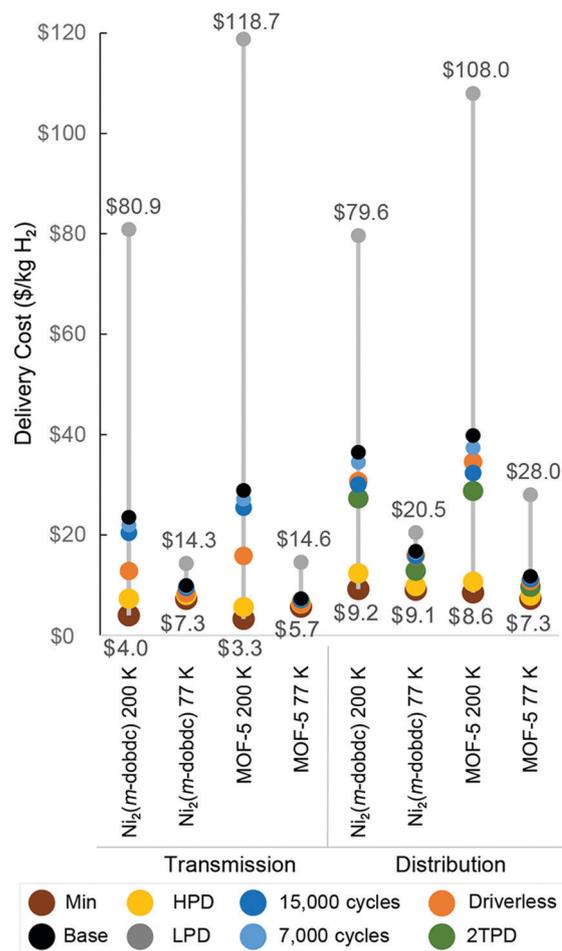

Fig. 5 Minimum (min), base case (base) and variations in H$_2$ transmission and distribution delivery costs for 50 000 kg H$_2$ per day including: driverless trucks, maximum number of cycles per MOF tube, low packing density tubes (LPD), high packing density tubes (HPD), and 2 trips per day (2TPD) to refueling stations. Marker sized varied for aesthetic purposes only.

assuming the deployment of best practices and research and development ongoing worldwide in adsorption and truck systems.

Employing driverless trucks would reduce the transmission cost of incumbent technologies by 21% (Comp-H$_2$-350 bar), 18% (Comp-H$_2$-500 bar), and 2% (Liq-H$_2$), while marginally reducing distribution costs (by 2–5%). In the case of MOF-H$_2$ systems, employing driverless trucks could reduce transmission costs by as much as 14 to 45%, relative to the base case, whereas distribution costs could be reduced by as much as 5 to 16%. Standards and industrial practices will play an important role in shaping the viability of any H$_2$ delivery technology. For example, if the number of allowable daily deliveries to refueling stations is increased from one to two, the distribution costs of the MOF-H$_2$ systems are reduced by as much as 18–28%.

In the most optimistic, "minimum cost" scenario shown in Fig. 5 for material performance and logistics, the market would be served by driverless trucks to lower labor costs, trailers would employ high packing density tubes that are stable to

1090 | Energy Environ. Sci., 2021, 14, 1083–1094

This journal is © The Royal Society of Chemistry 2021

15 000 cycles, and the cost of the MOF pellets remains $5 per kg. Under these conditions, the 200 K Ni$_2$(m-dobdc) and MOF-5 systems can be operated with minimum transmission costs of $4.0 and $3.3 per kg H$_2$, respectively for 100 km driving distances (Table S8, ESI†). While this minimum is still more expensive than Comp-H$_2$ delivery ($1.4 per kg H$_2$ for both pressures; Table S8, ESI†), it represents a significant 83–89% cost reduction relative to our base case cost scenario shown in Fig. 4, illustrating the substantial opportunities for improvement using adsorbent-based technology. In the case of Liq-H$_2$ and Comp-H$_2$ for both pressures, the minimum distribution and combined transmission–distribution costs differ by less than 10% from the base case costs in each scenario, suggesting that the performance of these technologies cannot be readily varied. An advantage of the MOF systems is the large range of energy and cost savings opportunities that could be achieved with improvements in technology and deployment experience.

Future system targets

Expanding from the scenarios developed above, there are a number of ways that our TEA model can be leveraged to explore the potential for MOF-H$_2$ delivery systems to be competitive and ultimately commercially viable in H$_2$ transport applications. For example, when considering just the tank-level, there is a cross-over point beyond which the quantity of H$_2$ adsorbed in Ni$_2$(m-dobdc) and MOF-5 at 77 K (low and high packing densities) becomes greater than the bulk H$_2$ in a Comp-H$_2$ system, considering pressures in the range of 1 to 500 bar (see Section 3.3 of the ESI† and Tables S9, S10). At 77 K and both packing densities, the Ni$_2$(m-dobdc) and MOF-5 tank systems cannot match the H$_2$ capacity achieved in a Comp-H$_2$ system.

We also considered a test case scenario where the performance of the Ni$_2$(m-dobdc)–H$_2$ system was evaluated for the three different supply chains when operated at 298 K and 250 bar. For this purpose, the Ni$_2$(m-dobdc) isotherm model was extrapolated to higher pressures and the same assumptions were used as those employed in the base case scenario (see Section 5 of the ESI†). These conditions were of interest as they would allow us to better understand the trade-off between H$_2$ uptake and compression and cooling costs. For a transmission distance of 100 km, the H$_2$ delivery cost is estimated to be $18.4 per kg H$_2$, of which $8.6 kg per H$_2$ is attributed to truck-related costs. Notably, 33% more H$_2$ is delivered per truck when compared with the Ni$_2$(m-dobdc)–H$_2$ system operated at 200 K and 100 bar, which translates to a 47% reduction in gas terminal costs and a 6% reduction in truck costs. However, as a result of the elevated pressure in this scenario, the tube cost ($19 147 per tube) is nearly three times that of the 100 bar tank system. In terms of the distribution value chain, the delivery cost for the base case is determined to be $34.5 per kg H$_2$ and is dominated by the costs of trucks and refueling station, which constitute 33% and 48% of the total cost, respectively. Despite the exploratory nature of this case study, the outcomes clearly stress the need for continued development of both adsorbents with higher uptake at ambient temperature and infrastructure

innovations that will lead to opportunities for even greater cost reductions.

Another alternative for setting system targets is to reverse engineer H$_2$ uptake based on the maximum allowable weight of the truck. Given a maximum allowable weight of 36 287 kg for the truck and fuel together[54] and subtracting the base truck weight of 12 596 kg, the allowable weight for nine tubes, the adsorbent, and H$_2$ is 23 691 kg. Based on this weight limit, it will be inherently challenging to meet the target weight percent in a bulk transportation application. For example, to outperform the H$_2$ storage capacity of a Comp-H$_2$-500 bar truck (800 kg), an ideal adsorbent material must possess a maximum gravimetric working capacity of at least 4.0 wt% (assuming a tube weight of 407 kg, which does not include any additional cooling equipment; see Section 1.4.1 of the ESI†), even under the assumption that H$_2$ is fully discharged within a prescribed timeframe. Based on the assumptions employed in the base case scenario and allowing for a tube weight of 407 kg, we estimate usable gravimetric capacities of 1.3 and 0.2 wt% at 77 and 200 K, respectively, for the Ni$_2$(m-dobdc)-filled tube system. In the case of MOF-5, the usable gravimetric capacities are estimated to be 2.7 and 0.2 wt% at 77 and 200 K, respectively. Thus, neither MOF system comes close to achieving the necessary gravimetric capacity to be competitive with current technology. Also, it is critical to stress that high H$_2$ uptake must be achieved in MOF systems at temperatures well above 77 K, because operation at this temperature would be too costly. Indeed, at 77 K the cost of refrigeration at the MOF-system gas terminal already exceeds the full delivery cost of both Comp-H$_2$ systems. At 200 K, the MOF-5-H$_2$ system would be competitive with the Liq-H$_2$ and the 350 and 500 bar Comp-H$_2$ systems for H$_2$ transmission if the adsorbent gravimetric capacity was increased from 0.2 wt% to 3.2, 9.8, and 10.8 wt%, respectively, holding the tube and adsorbent weight (as well as the costs of the terminal and tube-trailer precooling) constant; the gravimetric capacity of the Ni$_2$(m-dobdc)–H$_2$ system would need to be increased from 0.2 wt% to 2.5, 10.9, and 14 wt%, respectively.

Doubling the storage capacity of MOFs at ambient or near ambient temperature is a critical target of ongoing research sponsored by the DOE.[4,19] To this end, one approach is to design and synthesize MOFs featuring open metal sites that can bind multiple H$_2$ per site.[4,55,56] This strategy was recently demonstrated experimentally for the first time with the MOF Mn$_2$(dsbdc) (dsbdc^{4-} = 2,5-disulfido-1,4-benzenedicarboxylate), but only half of the manganese(II) ions in this material are capable of binding two H$_2$ molecules, and the corresponding binding energy is too low for room temperature storage (-5.6 kJ mol^{-1}).[57] Calculations have suggested that alkaline-earth ions can potentially bind multiple H$_2$ molecules with a higher binding enthalpy on the order of -20 kJ mol^{-1},[58] and thus the synthetic space for the development of such next-generation H$_2$ adsorbents for ambient temperature storage remains open for exploration. Importantly, the TEA model presented here can be used to analyze new H$_2$ adsorbents of interest for transportation applications, for example the recently reported framework NU-1501-Al, which exhibits a

This journal is © The Royal Society of Chemistry 2021

Energy Environ. Sci., 2021, 14, 1083–1094 | 1091

deliverable H_2 capacity of 14 wt% at 77 K.[59] Such a holistic approach—which accounts for upstream and downstream effects on cost resulting from MOF and adsorption tank performance---will be key to identifying future system targets for hydrogen storage for a range of applications, given that evaluating an H_2 adsorbent system at the tank level is likely to yield a very different view of H_2 storage performance than that derived from laboratory-scale experimental data.[60]

Concluding remarks

The foregoing study represents the first comprehensive analysis of the cost profile of different land-based H_2 supply chains and benchmarks prospective MOF-H_2 supply chain models with Comp-H_2 and Liq-H_2. Although the MOF-H_2 systems were found to be far costlier than the conventional H_2 delivery modes for all studied supply chains, it is important to note that Comp-H_2 trucks are not widely deployed at present, and this analysis does not capture safety considerations that inhibit the scale-up of Comp-H_2 storage. Lower pressure systems such as those using MOFs could reduce the risks associated with transporting a flammable gas such as H_2, but it is unclear to what extent this is practically true. While a full safety analysis is beyond the scope of this study, preliminary safety analysis conducted for MOF-based H_2 storage systems suggest these materials to be sufficiently safe.[43] Standards, codes, and regulations developed for either Comp-H_2 or Liq-H_2 technologies can be extended to the operating temperatures and pressures assumed for MOF-based truck systems in this study. Liquefied hydrogen can reduce the number of trucks congesting the roads for last-mile deliveries, but "micro-liquefaction" has yet to be fully commercialized, making downsizing of liquefaction facilities a challenge.

Under the most optimistic technical and market conditions, $Ni_2(m\text{-dobdc})$ or MOF-5 systems are capable of attaining a levelized H_2 transmission cost lower than that for Liq-H_2 and comparable to that for Comp-H_2 at 350 bar. Further reduction in adsorbent system costs could be achieved by increasing the delivered H_2 capacity per truck by increasing the deliverable capacity of the MOF, the MOF packing density, the maximum number of adsorption cycles per tube trailer, and the refueling station size. Although the potential for reaching these optimistic conditions requires practical testing, particularly of the modeled adsorption cycles and packing bed characteristics, our analysis provides important insights into the effect of the MOF material and adsorption column performance on system-wide costs. Indeed, more important than the specific systems considered here is the introduction of a widely applicable methodology that can be used to predict the viability of next-generation adsorbents for practical applications.

Future analysis would benefit from adsorption column data to better characterize the kinetics that drive H_2 sorption properties over time, which is in turn necessary for optimizing total system costs. Given that contaminants such as trace water can limit MOF cycling stability, it will also be important to identify purity requirements for different end uses. Additionally, there are currently few technologies that can be used to guide preliminary modeling of heat management and MOF cycling stability, and it will be important to determine whether adsorbents can be removed from the tubes at their end of life, or if the entire tube-trailer requires replacing. Better quantification of the H_2 losses that occur in all low-temperature systems is also needed. Conducting a heat transfer analysis would also be beneficial toward future development of an efficient refrigeration system for MOF-H_2 delivery technology that would enhance H_2 adsorption efficiency and lower overall energy costs.

Finally, energy savings could be attained with the discovery of H_2 storage materials that perform efficiently at ambient pressures, but only if new "last-mile" downstream infrastructure is concurrently advanced to enhance their competitiveness. Our results suggest that markets beyond the transportation sector are also worth investigating for any carrier material or chemical that delivers H_2 to refueling stations at moderate pressures. At a market price range for H_2 fuel ranging from $12.9 to $14.0 per kg,[52] it is apparent that for the MOF-based truck systems to be considered a competitive H_2 transportation technology, substantial improvements in the both the total deliverable H_2 capacity and the refueling station costs should be attained.

Conflicts of interest

There are no conflicts to declare.

Acknowledgements

References

1 International Energy Agency (IEA), The Future of Hydrogen: Seizing today's opportunities, 2019.

2 J. O. Abe, P. I. Popoola, E. Ajenifuj and O. M. Popoola, Hydrogen energy, economy and storage: Review and recommendation, *Int. J. Hydrogen Energy*, 2019, **44**, 15072–15086.

1092 | *Energy Environ. Sci.*, 2021, **14**, 1083–1094

This journal is © The Royal Society of Chemistry 2021

3   I. Staffell, *et al.*, The role of hydrogen and fuel cells in the global energy system, *Energy Environ. Sci.*, 2019, **12**, 463–491.

4   M. D. Allendorf, *et al.*, An assessment of strategies for the development of solid-state adsorbents for vehicular hydrogen storage, *Energy Environ. Sci.*, 2018, **11**, 2784–2812.

5   B. Zohuri, *Hydrogen Storage Processes and Technologies. in Hydrogen Energy*, Springer, 2019.

6   E. Rivard, M. Trudeau and K. Zaghib, Hydrogen storage for mobility: A review, *Materials*, 2019, **12**, 1973.

7   F. Zhang, P. Zhao, M. Niu and J. Maddy, The survey of key technologies in hydrogen energy storage, *Int. J. Hydrogen Energy*, 2016, **41**, 14535–14552.

8   C. Yang and J. Ogden, Determining the lowest-cost hydrogen delivery mode, *Int. J. Hydrogen Energy*, 2007, **32**, 268–286.

9   I. Lee, K. Tak, S. Lee, D. Ko and I. Moon, Decision Making on Liquefaction Ratio for Minimizing Specific Energy in a LNG Pilot Plant, *Ind. Eng. Chem. Res.*, 2015, **54**, 12920–12927.

10 B. J. Bucior, *et al.*, Energy-based descriptors to rapidly predict hydrogen storage in metal-organic frameworks, *Mol. Syst. Des. Eng.*, 2019, **4**, 162–174.

11 A. Ahmed, *et al.*, Balancing gravimetric and volumetric hydrogen density in MOFs, *Energy Environ. Sci.*, 2017, **10**, 2459–2471.

12 B. Hardy, *et al.*, Modeling of adsorbent based hydrogen storage systems, *Int. J. Hydrogen Energy*, 2012, **37**, 5691–5705.

13 D. DeSantis, *et al.*, Techno-economic analysis of metal–organic frameworks for hydrogen and natural gas storage, *Energy Fuels*, 2017, **31**, 2024–2032.

14 Argonne National Laboratory, Hydrogen Delivery Scenario Analysis Model (HDSAM).

15 G. Parks, R. Boyd, J. Cornish and R. Remick, *Hydrogen Station Compression, Storage, and Dispensing Technical Status and Costs: Systems Integration*, U.S. Department of Energy Hydrogen and Fuel Cells Program, 2014.

16 H. Li, M. Eddaoudi, M. O'Keeffe and O. M. Yaghi, Design and synthesis of an exceptionally stable and highly porous metal-organic framework, *Nature*, 1999, **402**, 276–279.

17 M. T. Kapelewski, *et al.*, M2(m-dobdc) (M = Mg, Mn, Fe, Co, Ni) metal-organic frameworks exhibiting increased charge density and enhanced H2 binding at the open metal sites, *J. Am. Chem. Soc.*, 2014, **136**, 12119–12129.

18 S. S. Kaye, A. Dailly, O. M. Yaghi and J. R. Long, Impact of preparation and handling on the hydrogen storage properties of Zn4O(1,4-benzenedicarboxylate)3 (MOF-5), *J. Am. Chem. Soc.*, 2007, **129**, 14176–14177.

19 M. T. Kapelewski, *et al.*, Record High Hydrogen Storage Capacity in the Metal − Organic Framework Ni2(m-dobdc) at Near-Ambient Temperatures, *Chem. Mater.*, 2018, **30**, 8179–8189.

20 R. Sathre, *et al.*, Life-cycle net energy assessment of large-scale hydrogen production via photoelectrochemical water splitting, *Energy Environ. Sci.*, 2014, **7**, 3264–3278.

21 S. Viscelli, *et al.*, *Autonomous Trucks and the Future of the American Trucker*, 2018.

22 P. Andersson and P. Ivehammar, Benefits and Costs of Autonomous Trucks and Cars, *J. Transp. Technol.*, 2019, **09**, 121–145.

23 Inc City Machine & Welding, Hydrogen Tube Trailer-9 Tubes DOT 3AAX 2400 PSI 40 FT, 2019.

24 Hydrogen Storage Engineering Center of Excellence (HSE-CoE), Tankinator.

25 T. Q. Hua, *et al.*, *Technical assessment of compressed hydrogen storage tank systems for automotive applications*, Argonne National Laboratory, 2010, DOI: 10.1016/j.ijhydene.2010.11.090.

26 *MATLAB and Statistics Toolbox Release*, The MathWorks, Inc., 2018.

27 S. A. Nouh, K. K. Lau and A. M. Shariff, Modeling and simulation of fixed bed adsorption column using integrated CFD approach, *J. Appl. Sci.*, 2010, **10**, 3229–3235.

28 A. Basu, *et al.*, A comprehensive approach for modeling sorption of lead and cobalt ions through fish scales as an adsorbent, *Chem. Eng. Commun.*, 2006, **193**, 580–605.

29 A. S. Yusuff, L. T. Popoola, O. O. Omitola, A. O. Adeodu and I. A. Daniyan, Mathematical Modelling of Fixed Bed Adsorption Column for Liquid Phase Solute: Effect of Operating Variables, *Int. J. Sci. Eng. Res.*, 2013, **4**, 811–822.

30 L. J. Wang, *et al.*, Synthesis and characterization of metal-organic framework-74 containing 2, 4, 6, 8, and 10 different metals, *Inorg. Chem.*, 2014, **53**, 5881–5883.

31 B. D. James, *2015 DOE Hydrogen and Fuel Cells Program Review: Hydrogen Storage Cost Analysis*, 2015.

32 D. Lenzen, *et al.*, A metal–organic framework for efficient water-based ultra-low-temperature-driven cooling, *Nat. Commun.*, 2019, **10**, 1–9.

33 R. K. Ahluwalia, *et al.*, Supercritical cryo-compressed hydrogen storage for fuel cell electric buses, *Int. J. Hydrogen Energy*, 2018, **43**, 10215–10231.

34 W. A. Amos, *Costs of Storing and Transporting Hydrogen*, 1998.

35 SA Prosim, ProsimPlus, 2020.

36 Argonne National Laboratory, Hydrogen Refueling Station Analysis Model (HRSAM), (2014).

37 US Department of Energy. DOE Technical Targets for Hydrogen Delivery.

38 A. Hooper and D. Murray, *An Analysis of the Operational Costs of Trucking: 2018 Update*, 2018.

39 B. D. James, *2015 DOE Hydrogen and Fuel Cells Program Review-Hydrogen Storage Cost Analysis*, 2015.

40 M. Wang, *et al.*, Hierarchical Porous Chitosan Sponges as Robust and Recyclable Adsorbents for Anionic Dye Adsorption, *Sci. Rep.*, 2017, **7**, 1–11.

41 Y. Yuan, *et al.*, Porous activated carbons derived from pleurotus eryngii for supercapacitor applications, *J. Nanomater.*, 2018, **2018**, 10.

42 H. Xu, *et al.*, Nanoporous activated carbon derived from rice husk for high performance supercapacitor, *J. Nanomater.*, 2014, **2014**, 8.

43 M. Veenstra, *Ford/BASF-SE/UM Activities in Support of the Hydrogen Storage Engineering Center of Excellence*, 2015.

This journal is © The Royal Society of Chemistry 2021

Energy Environ. Sci., 2021, **14**, 1083–1094 | 1093

44 B. Schmitz, et al., Heat of adsorption for hydrogen in microporous high-surface-area materials, *ChemPhysChem*, 2008, **9**, 2181–2184.

45 D. Lefebvre, P. Amyot, B. Ugur and F. H. Tezel, Adsorption Prediction and Modeling of Thermal Energy Storage Systems: A Parametric Study, *Ind. Eng. Chem. Res.*, 2016, **55**, 4760–4772.

46 T. W. Weber and R. K. Chakravorti, Pore and solid diffusion models for fixed-bed adsorbers, *AIChE J.*, 1974, **20**, 228–238.

47 D. Papurello, M. Gandiglio and A. Lanzini, Experimental analysis and model validation on the performance of impregnated activated carbons for the removal of hydrogen sulfide (H2S) from sewage biogas, *Processes*, 2019, **7**, 1–26.

48 Y. Taamneh and R. Al Dwairi, The efficiency of Jordanian natural zeolite for heavy metals removal, *Appl. Water Sci.*, 2013, **3**, 77–84.

49 F. Ventriglio, D. M. Zall, C. J. Stockhausen and D. Decker, *Carbon dioxide sorbent for confined breathing atmospheres*, 1973.

50 R. Paggiaro, P. Bénard and W. Polifke, Cryo-adsorptive hydrogen storage on activated carbon. I: Thermodynamic analysis of adsorption vessels and comparison with liquid and compressed gas hydrogen storage, *Int. J. Hydrogen Energy*, 2010, **35**, 638–647.

51 Ballard Power Systems & Nel Hydrogen, Hydrogen at Scale for Fuel Cell Electric Buses A California Case Study, 2019.

52 California Energy Commission, Joint Agency Staff Report on Assembly Bill 8: Assessment of Time and Cost Needed to Attain 100 Hydrogen Refueling Stations in California, 2015.

53 California Fuel Cell Partnership, What Do You Need To Know About Hydrogen Fueling Operations? 2015.

54 US Department of Transportation, Freight Management and Operations, 2017.

55 P. Agarwala, S. K. Pati and L. Roy, Unravelling the possibility of hydrogen storage on naphthalene dicarboxylate-based MOF linkers: a theoretical perspective, *Mol. Phys.*, 2020, **8976**, e1757169.

56 D. P. Broom, et al., Concepts for improving hydrogen storage in nanoporous materials, *Int. J. Hydrogen Energy*, 2019, **44**, 7768–7779.

57 T. Runčevski, et al., Adsorption of two gas molecules at a single metal site in a metal-organic framework, *Chem. Commun.*, 2016, **52**, 8251–8254.

58 E. Tsivion, S. P. Veccham and M. Head-Gordon, High-Temperature Hydrogen Storage of Multiple Molecules: Theoretical Insights from Metalated Catechols, *ChemPhysChem*, 2017, **18**, 184–188.

59 Z. Chen, et al., Balancing volumetric and gravimetric uptake in highly porous materials for clean energy, *Science*, 2020, **368**, 297–303.

60 B. P. Prajwal and K. G. Ayappa, Evaluating methane storage targets: From powder samples to onboard storage systems, *Adsorption*, 2014, **20**, 769–776.

1094 | *Energy Environ. Sci.*, 2021, **14**, 1083–1094

This journal is © The Royal Society of Chemistry 2021